

25 **Abstract**

26 Dark fermentative biohydrogen production in a thermophilic, xylose-fed (50 mM) fluidised bed
27 reactor (FBR) was evaluated in the temperature range 55–70 °C with 5-degree increments and
28 compared with a mesophilic FBR operated constantly at 37 °C. A significantly higher ($p = 0.05$) H₂
29 yield was obtained in the thermophilic FBR, which stabilised at about 1.2 mol H₂ mol⁻¹ xylose (36%
30 of the theoretical maximum) at 55 and 70 °C, and at 0.8 mol H₂ mol⁻¹ xylose at 60 and 65 °C,
31 compared to the mesophilic FBR (0.5 mol H₂ mol⁻¹ xylose). High-throughput sequencing of the
32 reverse-transcribed 16S rRNA, done for the first time on biohydrogen producing reactors, indicated
33 that *Thermoanaerobacterium* was the prevalent active microorganism in the thermophilic FBR,
34 regardless of the operating temperature. The active microbial community in the mesophilic FBR was
35 mainly composed of *Clostridium* and *Ruminiclostridium* at 37 °C. Thermophilic dark fermentation
36 was shown to be suitable for treatment of high temperature, xylose-containing wastewaters, as it
37 resulted in a higher energy output compared to the mesophilic counterpart.

38

39 **Keywords:** Active community, Biohydrogen, FBR, MiSeq, *Thermoanaerobacterium*, Thermophilic

40

41

42

43

44

45

46

47

48

49

50 **1. Introduction**

51 H₂ is a carbon free fuel considered as a promising candidate to replace fossil fuels in the near future
52 [1]. Although hydrocarbons are currently the main feedstock for H₂ production, biomass is a
53 renewable and environmentally friendly alternative feedstock [2]. Dark fermentation is the most
54 studied among the biological H₂ production technologies because the variety of usable organic
55 substrates, and the high achievable conversion rates, may promote the scale-up of the process [3].
56 However, due to the thermodynamics of the reactions involved, which are more favourable at high
57 temperature and low H₂ partial pressure, operation and optimisation of full-scale dark fermentation
58 is more challenging than traditional anaerobic digestion [4].

59

60 Many pathways are possible for dark fermentation, depending on the microbial species, operating
61 parameters, and the substrate used. Glycolysis is the most common route for degradation of hexoses
62 by *Clostridium* [5] and most thermophiles, including *Thermoanaerobacter* [6]. Glucose is oxidised
63 to pyruvate, resulting in the generation of reduced nicotinamide adenine dinucleotide (NADH) and
64 energy in the form of adenosine triphosphate [7]. Pyruvate may be further oxidised to acetylcoenzyme
65 A through reduction of ferredoxin and then to volatile fatty acids (VFAs), or alcohols [7].
66 Metalloenzymes called hydrogenases use NADH or reduced ferredoxin as electron donor for proton
67 oxidation [8], resulting in the formation of molecular H₂. The oxidation of glucose to H₂ and CO₂
68 yields 12 mol H₂ mol⁻¹ glucose. However, the dehydrogenation of acetate to CO₂ is endergonic, and
69 the spontaneous oxidative process will thus end with acetate production, yielding only 4 mol H₂ mol⁻¹
70 glucose [9]. This thermodynamic limitation is also valid for pentose sugars such as xylose, which
71 will then yield a maximum of 3.33 mol H₂ mol⁻¹ xylose.

72

73 In practice, the H₂ yield by mixed cultures varies from 14% to 70% of the theoretical limit [10]. For
74 high H₂ partial pressures (> 60 Pa), proton reduction by NADH is not thermodynamically favourable

75 and the reaction switches, e.g. to the butyrate pathway [11], resulting in a lower H₂ yield. Temperature
76 and pH also strongly affect the microbial community and thus, the substrate degradation pathway
77 [12]. Butyrate accumulation can trigger solventogenesis [13], which does not yield H₂. Some
78 microorganisms, including various *Clostridium* sp., are facultative autotrophic and can reduce CO₂
79 with H₂ forming acetate [10]. Other known H₂-consuming microorganisms include hydrogenotrophic
80 methanogens, propionate producers, and sulfate or nitrate reducing bacteria [14].

81

82 H₂ production at high temperatures can be advantageous in terms of H₂ yield and production rates
83 [15,16]. High temperature positively affects the kinetics of the oxidative reactions and the growth of
84 microorganisms [17]. Furthermore, the direct conversion of sugars to acetate becomes
85 thermodynamically more favourable as the temperature increases, thus resulting in a high H₂ yield
86 [18]. Thermophilic anaerobic microorganisms such as *Thermotoga* and *Thermoanaerobacter* are
87 excellent H₂ producers, as they use most of the reductants produced during glycolysis to form H₂,
88 allowing yields between 3 and 4 mol H₂ mol⁻¹ hexose [18]. Although H₂ yields from pure cultures are
89 typically higher [5], mixed cultures are preferable for industrial application, as they offer more
90 stability and versatility, and sterilisation is not required [12]. Most studies on H₂ production at high
91 temperature by mixed cultures have been conducted at 55, 60, or 70 °C, generally obtaining higher
92 H₂ yields than mesophilic trials with a similar inoculum and substrate [16,19,20].

93

94 Handling and processing of organic substrates and the low H₂ yield are two of the main deterrents for
95 the establishment of dark fermentation at commercial scale [21]. Despite the high H₂ yield obtained
96 at high temperatures, the net energy gain (the difference between the energy input needed to heat the
97 reactor and output) seems to be indirectly proportional to the operation temperature [22]. However,
98 some industrial wastewaters, such as thermomechanical pulping wastewaters, are produced at high
99 (50–70 °C) temperatures [23] and could be treated in situ avoiding cooling and minimising energy

100 loss. Such wastewaters contain readily fermentable sugars, both hexoses (mainly glucose) and
101 pentoses (mainly xylose), suitable for H₂ production by dark fermentation. Continuous dark
102 fermentation of glucose has been widely studied at various temperatures [24–28], while much less
103 attention was given to dark fermentation of xylose, especially at high temperature. In a previous study,
104 H₂ production from xylose was compared in batch cultures at 37, 55 and 70 °C, using heat treated (90
105 °C, 15 min) activated sludge from a wastewater treatment plant as the inoculum [16]. That study
106 showed effective H₂ production at 55 °C, but not at 70 °C. However, the effect of temperature in the
107 55–70 °C temperature range is worth investigating, as a difference of a few degrees can affect the
108 microbial community inside the reactor and thus, the H₂ production efficiency [28].

109
110 Recently, the establishment of next-generation sequencing techniques has improved the knowledge
111 on H₂-producing microbial communities. Etchebehere et al. [29] performed 454 pyrosequencing on
112 microbiological samples from 20 H₂ producing lab-scale bioreactors operated within a temperature
113 range of 25–37 °C. Although the microbial communities were diverse due to the different operating
114 conditions of the bioreactors, the authors observed a predominance of *Firmicutes* and distinguished
115 high-yield H₂ producers (*Clostridium*, *Kosmotoga*, and *Enterobacter*), low-yield H₂ producers
116 (*Veillonellaceae*) and competitors (*Lactobacillus*). Nitipan et al. [30] reported
117 *Thermoanaerobacterium* as the dominant genus in a thermophilic (60 °C) sequencing batch reactor
118 producing H₂ from palm oil mill effluent. Zhang et al. [31] showed that *Firmicutes* such as
119 *Caldanaerobius*, *Caldicellulosiruptor*, and *Thermoanaerobacter* become dominant in a
120 hyperthermophilic (70 °C) H₂ producing, glucose-fed chemostat. To date, analysis of dark
121 fermentative microbial communities by next-generation sequencing has been mainly based on the
122 presence of 16S rRNA genes, which provide information on the structure of the microbial community.
123 However, an analysis based on the expression of 16S rRNA genes describes more accurately the
124 composition of the microbial community actively involved in dark fermentation [32].

125

126 This study aims to evaluate, for the first time, how dark fermentative H₂ production and the
127 composition of the active microbial community are affected by a stepwise (5 °C) temperature increase
128 in the 55–70 °C temperature range in a xylose-fed fluidised bed reactor (FBR) inoculated with heat
129 treated activated sludge. A second FBR was operated in parallel with the same inoculum, but at a
130 lower temperature (37 °C) in order to compare its performance to the thermophilic counterpart, prior
131 to increasing the temperature to 55 °C to observe the response of this mesophilic microbial
132 community to the temperature shift.

133

134 **2. Materials and methods**

135 *2.1 Source of biomass*

136 Activated sludge was collected from the recirculation line between the aeration tank and the
137 secondary settler in the Viinikanlahti municipal wastewater treatment plant (Tampere, Finland). It
138 was settled, and, after removing the supernatant, heat-treated at 90 °C for 15 minutes as described by
139 Dessì et al. [16] before being used as inoculum for the FBRs.

140

141 *2.2 Composition of synthetic wastewater*

142 Both FBRs were fed with a synthetic wastewater based on the DSMZ 144 medium, with xylose (50
143 mM) as electron donor instead of glucose. However, tryptone, resazurin and Na₂S were omitted and
144 the concentration of KH₂PO₄, K₂HPO₄, and yeast extract was reduced 10 times (to 0.55 mM, 0.86
145 mM, and 0.3 g L⁻¹, respectively).

146

147 *2.3 FBR configuration*

148 Two FBRs (Figure 1), 1 L volume each, were operated with 300 mL activated carbon as carrier
149 material for biomass adhesion. A recirculation flow rate of about 1900 mL min⁻¹ was applied by using

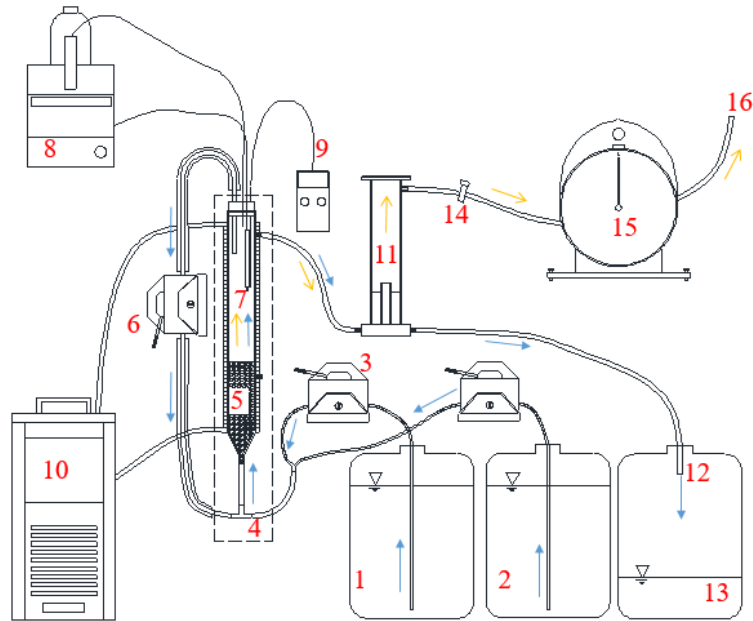
150 a peristaltic pump (Masterflex, USA) to expand the activated carbon bed by 30% (the flow rate of
151 minimum fluidization was 1400 mL min⁻¹). To maintain a constant expansion, the recirculation flow
152 was increased up to a maximum of 20% due to the adhesion of the biomass, which made the bed
153 heavier. To achieve a stable temperature, the FBRs were operated inside incubators (Labilo, Finland).
154 A water jacket (Julabo, Germany) was also installed, as the heat provided by the incubator was not
155 enough to reach 70 °C inside the FBR.

156

157 To avoid microbial growth, the xylose solution was prepared in a different tank than the medium
158 containing the nutrients and trace elements. Both solutions were flushed with N₂ into the feeding
159 tanks, and their pH was adjusted to 5.0–5.5 with HCl prior to being fed to the FBRs through peristaltic
160 pumps (Masterflex, USA). To minimise the growth of methanogenic archaea [33], the pH inside the
161 reactor was kept at 5 (± 0.1) by automatic titration (Metrohm, Switzerland). The FBRs were sealed
162 on the top, and both liquid and gas were directed to a gas-liquid separator. The liquid was directed to
163 an effluent tank, while the gas was directed to a gas meter (Ritter, Germany) before being released
164 into a fume hood (Figure 1).

165

166



167

168 **Figure 1.** Overview of the experimental set-up used in this study. Medium influent tank (1), xylose
 169 influent tank (2), peristaltic pumps for influent feeding (3), influent sampling point (4), activated
 170 carbon bed with the active biomass (5), peristaltic pump for recirculation (6), pH probe (7), automatic
 171 titrator (8), temperature control (9), water jacket (10), gas-liquid separator (11), effluent sampling
 172 point (12), effluent tank (13), gas sampling point (14), gas meter (15), and gas outlet (16). Liquid path
 173 (↗), gas path (↘). The dashed rectangle represents the part of the set-up located inside the
 174 incubator.

175

176 2.4 FBR operation and sampling

177 Both FBRs were inoculated by 50 mL of heat-treated activated sludge (8.8 g VS L⁻¹). After two days
 178 of start-up in batch mode, the FBRs were switched to continuous mode (day 0) and operated for 7
 179 days at a hydraulic retention time (HRT) of 12 hours. On day 7, the HRT was decreased to 6 hours.
 180 The thermophilic FBR was operated in continuous mode for a total of 185 days. It was initially
 181 operated at 55 (± 1) °C. Temperature was then increased to 60 (± 1) °C on day 77, to 65 (± 1) °C on
 182 day 119, and to 70 (± 1) °C on day 158 until day 185. The mesophilic FBR was operated at 37 (± 1)
 183 °C for 185 days, and then at 55 (± 1) °C until day 228.

184

185 Influent and effluent samples, and gas samples, were collected from the sampling points specified in
186 Figure 1. Biofilm-containing activated carbon was collected from the thermophilic FBR before every
187 change in operating conditions (plus a mid-term sample collected on day 53), and stored at -20 °C for
188 DNA analysis. Samples from the mesophilic FBR were also collected on the same days. An additional
189 sample of carrier material was collected from the thermophilic FBR on day 119 (60 °C), 158 (65 °C),
190 and 185 (70 °C) and, from the mesophilic reactor on day 185 (37 °C), and 228 (55 °C), and stored at
191 -80 °C for RNA-level analysis. The collection system consisted of a syringe connected to a tube,
192 which was used to suck 4–6 mL biomass out of the FBR bed. While collecting the biomass samples,
193 the FBRs were open from the top but flushed with N₂ to avoid exposure to air.

194

195 *2.5 Chemical analysis*

196 Influent and effluent composition was determined either with GC-FID according to Kinnunen et al.
197 [34], or with HPLC as reported by Dessì et al. [16]. Gas samples were analysed for H₂, CH₄, and CO₂
198 with a Shimadzu gas chromatograph GC-2014 equipped with a Porapak N column (80/100 mesh) and
199 a thermal conductivity detector. Oven, injector and detector temperatures were at 80, 110 and 110 °C,
200 respectively.

201

202 *2.6 Microbiological analysis*

203 DNA extraction and polymerase chain reaction-denaturing gradient gel electrophoresis (PCR-DGGE)
204 of the partial 16S rRNA gene were performed according to Mäkinen et al. [35]. The forward and
205 reverse primers for PCR were GC-BacV3f and 907r, respectively. The visible bands in the
206 polyacrylamide gel were cut by using a surgical blade, eluted in sterile water and re-amplified by
207 PCR (primers BacV3f and 907r) before sending them to Macrogen (South Korea) for sequencing as
208 described by Koskinen et al. [36]. The nucleotide sequences obtained were analysed using Bio-Edit

209 [37] software version 7.2.5, and compared with the sequences in the GenBank nucleotide collection
210 database using BLAST software [38].

211

212 Nucleic acids for MiSeq analysis were co-extracted from the biofilm-containing activated carbon
213 samples according to Griffiths et al. [39], but 3M sodium acetate (1/10 of sample volume) and cold
214 (-20 °C) 100% isopropanol (1 sample volume) were added for precipitation instead of polyethelene
215 glycol. Furthermore, nucleic acids were re-suspended in sterile water instead of tris-EDTA buffer.
216 DNA and RNA were quantified by a Nanodrop spectrophotometer (NanoDrop Technologies, USA).
217 Their quality was assessed by measuring the absorbance ratio at 260/280 nm, and 260/230 nm
218 wavelength. Nucleic acid samples were diluted to a final concentration of 25 ng mL⁻¹. DNA was
219 removed by adding 1 µL turbo DNase and 2.5 µL turbo DNase buffer (Invitrogen, Thermo Fisher,
220 USA), followed by incubation at 37 °C for 30 minutes. DNase was then inactivated by addition of
221 2.5 µL DNase inactivator (Invitrogen). After centrifugation (10000xg, 1.5 minutes), the RNA-
222 containing supernatant was transferred to a fresh RNase free tube. The absence of DNA was
223 confirmed by 16S rRNA gene PCR (primers 338f and 805r) followed by electrophoresis in 1%
224 agarose gel (no bands obtained). Complementary DNA (cDNA) was obtained from RNA using M-
225 MuLV Reverse Transcriptase (New England, BioLabs, USA), following the instructions provided by
226 the supplier. The success of the reverse transcription was confirmed by 16S rRNA gene PCR (primers
227 338f and 805r) and electrophoresis in 1% agarose gels (bands appeared). Samples of cDNA were sent
228 to FISABIO (Valencia, Spain) for high-throughput sequencing of partial 16S rRNA genes on an
229 Illumina MiSeq platform. Forward and reverse primers for PCR were 515f and 806r, respectively
230 [40]. A total of 427,163 raw sequences was obtained from 5 samples. Sequence screening, alignment
231 to Silva (v123) database, clustering, chimeras removal and taxonomic classification (cut-off = 97%)
232 were performed using Mothur v1.39.3 [41], following the procedure described by Kozich et al. [42].

233

234 2.7 Net energy gain calculation

235 The net energy gain (kJ L^{-1}) (Equation 2) was estimated by the sum of the energy recovered by
236 combustion of the H_2 produced per litre of wastewater treated (Equation 3) and the energy required
237 to heat the FBR to the desired temperature (Equation 4) [22]:

238

$$239 \text{ Net energy gain: } NE_G = E_G + E_L \quad (2)$$

$$240 \text{ Energy gain: } E_G = Y_H \cdot MV_H \cdot C_X \cdot \rho_H \cdot LHV_H \quad (3)$$

$$241 \text{ Energy loss: } E_L = C_W \cdot (T_F - T_I) \cdot \rho_W \quad (4)$$

242

243 where Y_H is the H_2 yield ($\text{mol H}_2 \text{ mol}^{-1}$ xylose), MV_H is the molar volume of H_2 ($22.414 \text{ L mol}^{-1}$), C_X
244 is the influent xylose concentration (50 mol L^{-1}), ρ_H is the density of gaseous H_2 ($8.9 \times 10^{-5} \text{ kg L}^{-1}$),
245 LHV_H is the lower heating value of H_2 ($120 \times 10^3 \text{ kJ kg}^{-1}$), C_W is the specific heat of water (4.2 kJ
246 $\text{kg}^{-1} \text{ K}^{-1}$), T_F and T_I (K) is the temperature of the wastewater after and before heating, respectively,
247 and ρ_W is the density of water (1 kg L^{-1}).

248

249 2.8 Statistical analysis

250 To assess significant differences in H_2 yield at the various temperatures investigated, analysis of
251 variance (ANOVA) and the Tukey test [43] at $p = 0.05$ were conducted using the IBM SPSS Statistics
252 package. The statistical analysis was conducted on the last 4 sampling points collected at the various
253 temperatures investigated in both the mesophilic and thermophilic FBR (8-10 operation days). The
254 output of the statistical analysis is provided in the supporting material (File S1).

255

256 3. Results

257 3.1 H_2 production in the thermophilic FBR

258 For all the temperatures investigated, the thermophilic FBR yielded more H₂ than the mesophilic FBR
259 (Figure 2a versus 2b). At 55 °C (days 1-77), the H₂ yield increased steadily in the first days of
260 operation, reaching 1.2 mol H₂ mol⁻¹ xylose on day 18, and remaining relatively stable on days 18–
261 25 (Figure 2a). In the following days, due to a problem with the liquid-gas separator (foam produced
262 by the FBR partially clogged the gas line and part of the gas was likely lost with the effluent), the H₂
263 yield decreased reaching a minimum of 0.7 mol H₂ mol⁻¹ xylose on day 35. On day 52, after solving
264 the issue by washing the liquid-gas separator, the H₂ yield increased sharply reaching a maximum of
265 about 1.3 mol H₂ mol⁻¹ xylose on day 56 and then stabilising to 1.2 mol H₂ mol⁻¹ xylose on days 65–
266 77 (Figure 2a). On days 7–77, xylose was detected in the effluent at a concentration < 2.5 mM (>
267 95% removal). Acetate and butyrate were the main metabolites produced. Their concentration in the
268 effluent increased on days 1–21, reaching a concentration of about 30 and 35 mM for acetate and
269 butyrate, respectively (Figure 2c). Ethanol was produced in the first days of operation, reaching a
270 maximum concentration of about 10 mM on day 7 before decreasing to < 2 mM on day 27. On days
271 65–77, the acetate concentration ranged between 20 and 24 mM, while the butyrate concentration
272 ranged between 19 and 25 mM (Figure 2c).

273

274 After increasing the temperature to 60 °C on day 77, the H₂ yield remained stable at 1.2 mol H₂ mol⁻¹
275 xylose for one day and then decreased to a minimum of 0.6 mol H₂ mol⁻¹ xylose on day 81 (Figure
276 2a). H₂ remained low on days 81–91 and started to increase again, reaching a maximum of about 1.0
277 mol H₂ mol⁻¹ xylose on day 95. From day 98, the H₂ yield slightly decreased again and stabilised to
278 0.8 mol H₂ mol⁻¹ xylose on days 112-119 (Figure 2a). The increase in temperature caused an increase
279 in the VFAs concentration in the effluent (Figure 2c). The acetate concentration almost doubled,
280 ranging between 29 and 42 mM on days 88–119. The butyrate concentration increased as well,
281 ranging between 25 and 35 mM on days 88–119 (Figure 2c).

282

283 At 65 °C (days 120–158), the average H₂ yield was comparable to the yield obtained at 60 °C, but the
284 production was more unstable compared to both 55 °C and 60 °C, ranging between 0.7 and 1.3 mol
285 H₂ mol⁻¹ xylose (Figure 2a). Increasing the temperature to 65 °C had minimal impact on the VFA
286 concentration when compared to the 60 °C condition (Figure 2c).

287

288 After increasing the temperature further to 70 °C, H₂ production ceased on day 161, but increased
289 again from day 163, stabilising to values comparable to those obtained at 55 °C (1.2 mol H₂ mol⁻¹
290 xylose) on days 172–185 (Figure 2a). A high concentration of xylose was detected in the effluent on
291 days 163–174, with a peak of about 50 mM (0% removal) on day 163. On days 163–174, the acetate
292 and butyrate concentration decreased and slowly increased again, reaching values comparable to the
293 ones obtained at 60 and 65 °C (21–32 mM acetate and 22–32 mM butyrate) on days 175–185 (Figure
294 2c).

295

296 *3.2 H₂ production in the mesophilic FBR*

297 The mesophilic FBR had a fluctuating H₂ production, especially during days 1–90. The H₂ yield was
298 above 1.0 mol H₂ mol⁻¹ xylose only on days 53–65. On day 7, 74 and 81, the H₂ yield ceased and
299 increased again within 1–3 days. On days 90–185, the H₂ production fluctuated between 0.3 and 1.0
300 mol H₂ mol⁻¹ xylose. Between days 0–185, the xylose concentration in the effluent was < 5 mM (>
301 90% removal).

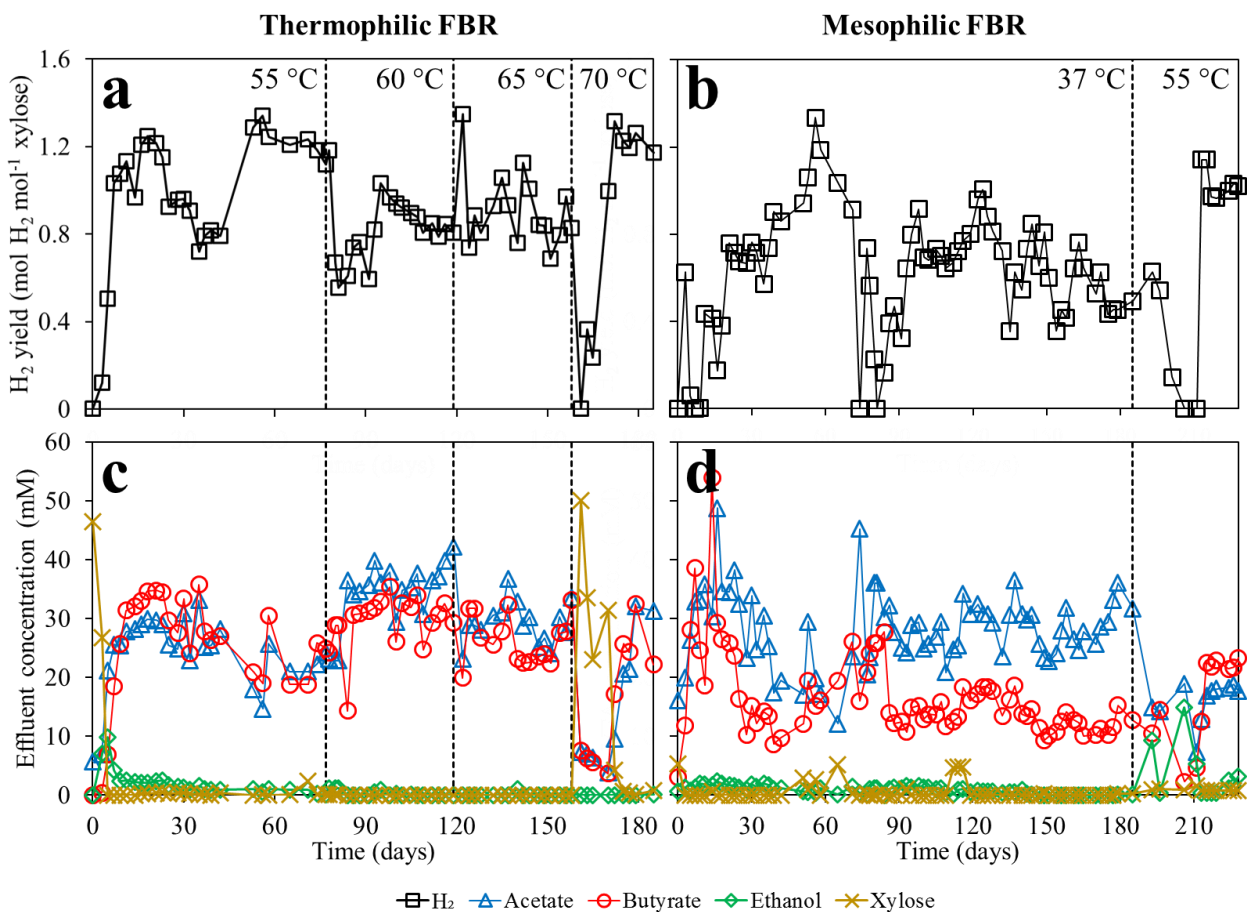
302

303 Similar to the H₂ yield, acetate and butyrate production was unstable during days 1–90 (Figure 2d).
304 The acetate concentration was often close to 40 mM and was even higher on day 18 and 76.
305 Interestingly, the peaks of acetate (Figure 2d) seem to mirror the drops in H₂ yield (Figure 2b). On
306 days 90–185, the butyrate concentration ranged between 10 and 19 mM, while the acetate
307 concentration was more unstable, ranging between 20 and 36 mM (Figure 2d).

308

309 After increasing the temperature to 55 °C (day 186), H₂ production ceased on day 206 (Figure 2b),
310 and then increased sharply to values comparable to those obtained in the thermophilic FBR at 55 °C
311 on days 219-228 (1.0 mol H₂ mol⁻¹ xylose). After raising the temperature from 37 to 55 °C, xylose
312 was still consumed (> 97%). Ethanol was detected in the effluent on days 195–213, with a maximum
313 of 15 mM on day 208 (Figure 2d). However, the liquid phase composition was similar to the one
314 obtained in the thermophilic FBR at 55 °C on days 217–228 (about 18 and 22 mM acetate and
315 butyrate, respectively).

316



317

318 **Figure 2.** H₂ yield (mol H₂ mol⁻¹ xylose added) (a, b) and acetate, butyrate, ethanol and xylose
319 concentration (mM) in the effluent (c, d) of the thermophilic (a, c) and mesophilic (b, d) FBR. The
320 vertical dotted lines indicate a change of temperature.

321

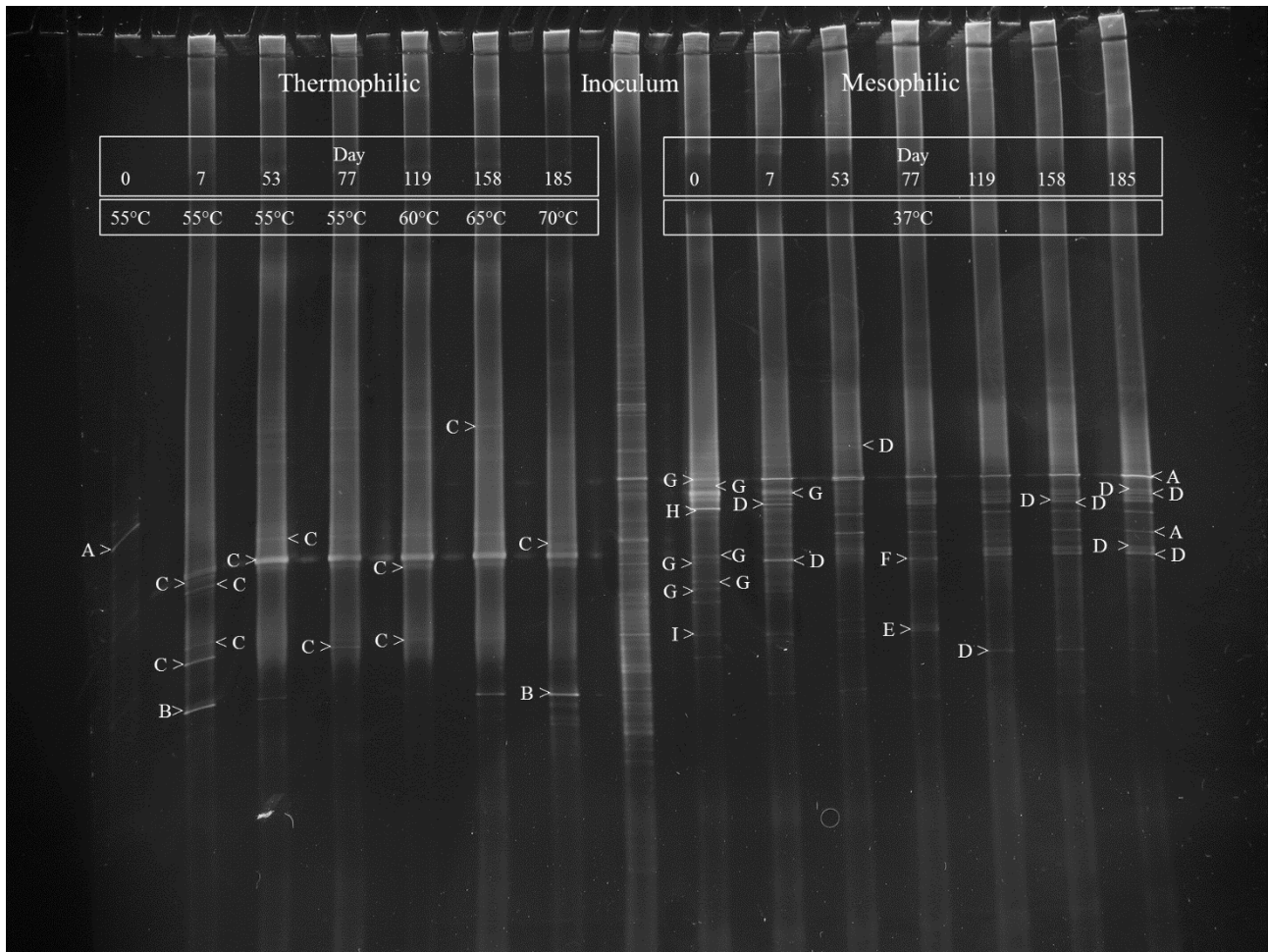
322 3.3 Microbial community analysis

323 Different eubacterial community profiles from the thermophilic and mesophilic FBR were obtained
324 by PCR-DGGE analysis from the biofilm-containing activated carbon (Figure 3; Table 1). In the
325 thermophilic FBR, *Clostridium acetobutylicum* (100% similarity) was found at 55 °C on day 0 (after
326 two days of start-up in batch mode), but was not detected in subsequent samples (Figure 3). On days
327 7–185, regardless the temperature, *Thermoanaerobacter thermosaccharolitycum* (98–99% similarity)
328 was the dominant microorganism in the thermophilic FBR (Figure 3). *Alicyclobacillus* sp. (96–97%
329 similarity) was found on day 7, after which its concentration was below detection limit at 55 °C on
330 day 77 and at 60 °C on day 119, but it was detected again when temperature was further increased to
331 65 and 70 °C (Figure 3).

332

333 A wider eubacterial community was found in the mesophilic FBR compared to the thermophilic FBR.
334 On day 0 and day 7, nucleotide sequences with 99–100% similarity to *Clostridium pasteurianum*
335 were detected. Species with 99–100% similarity to *Clostridium acetobutylicum* were detected on all
336 sampling days (days 7–185). On day 77, nucleotide sequences close to *Pseudomonas* and *Delftia* sp.
337 were also found. On days 119, 158, and 185, the DGGE profiles of the mesophilic community were
338 similar to each other and dominated by *Clostridium* sp. (Figure 3).

339



340

341 **Figure 3.** Microbial community profiles obtained by PCR–DGGE from biofilm-containing activated
 342 carbon samples collected from the thermophilic and the mesophilic H₂ producing FBR. The band
 343 labels refer to Table 1.

344

345

346

347

348

349

350

351

352

353 **Table 1.** Association of 16S rRNA gene sequences of DGGE bands to those collected in the GenBank.

BL^a	Affiliation^b	Accession number	Matching sequence length^c	Similarity (%)^d
A	<i>Clostridium acetobutylicum</i>	KP410577 KP410579	446–472	99–100
B	<i>Alicyclobacillus</i> sp.	JX505129	485–524	96–97
C	<i>Thermoanaerobacter thermosaccharolyticum</i>	JX984968 KJ831072 AF247003	405–499	98–99
D	<i>Clostridium</i> sp.	EU887966 EU887970 KU886097 LC020495	367–491	94–99
E	<i>Pseudomonas</i> sp.	GQ903481	442	97
F	<i>Delftia</i> sp.	KT865666	465	99
G	<i>Clostridium pasteurianum</i>	KX378861	440–506	99–100
H	<i>Ralstonia</i> sp.	KT183537	496	99
I	<i>Lysobacter</i> sp.	JQ791571	429	93

354 ^a Band label in Figure 3a

355 ^b Closest cultured species in GenBank

356 ^c Number of nucleotide pairs used in the sequence comparison

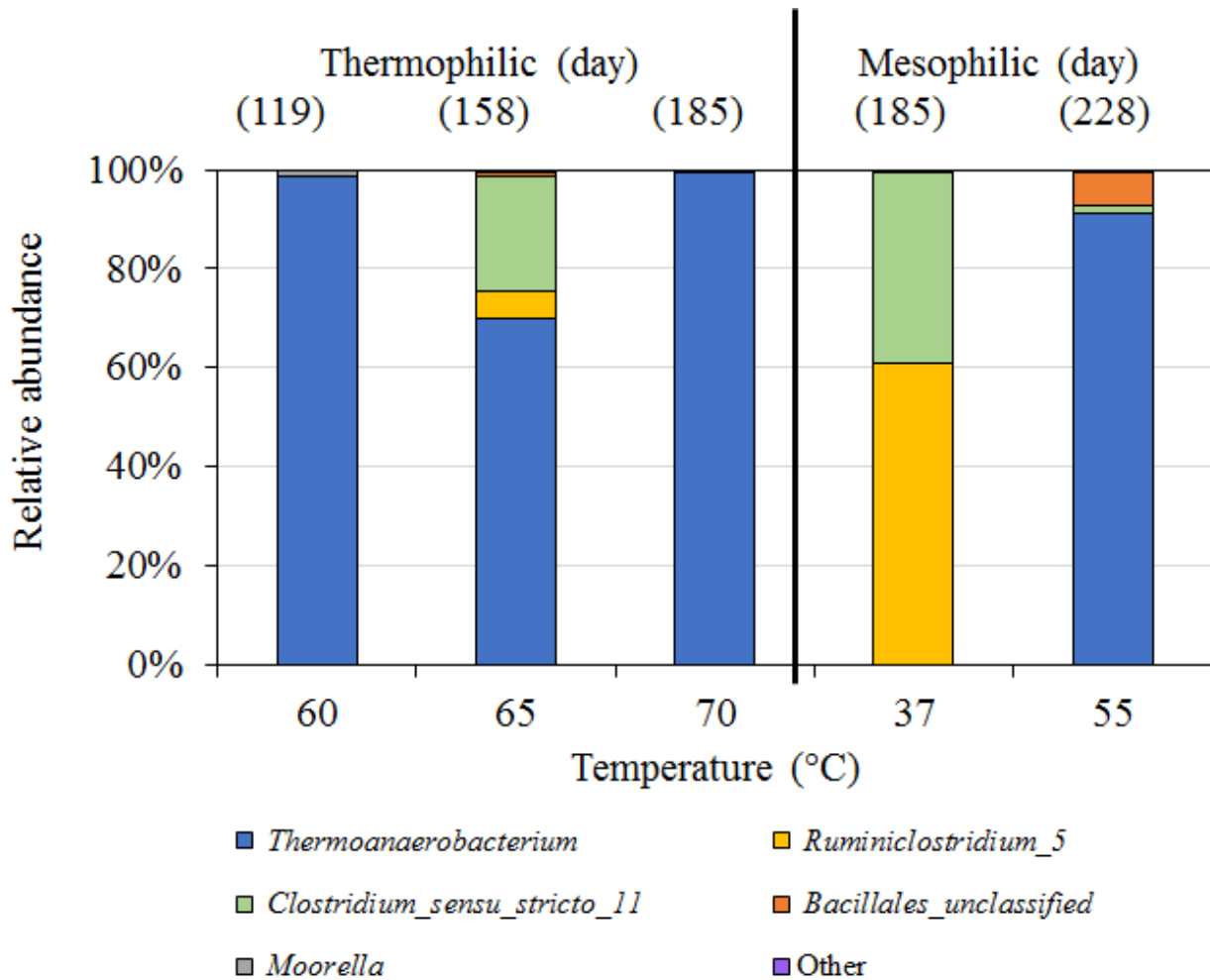
357 ^d Percentage of identical nucleotide pairs between the 16S rRNA gene sequence and the closest species in GenBank

358

359 Based on the high-throughput sequencing of the reverse-transcribed 16S rRNA (Figure 4), species
 360 belonging to the *Thermoanaerobacterium* genus dominated the active microbial community (> 99%
 361 of the relative abundance) of the thermophilic FBR at both 60 and 70 °C (days 119 and 185). At 65
 362 °C (day 158), about 22% of the relative abundance matched the genus *Clostridium* (Figure 4). In the
 363 mesophilic FBR, microorganisms of the genus *Clostridium* and *Ruminiclostridium* dominated the

364 active microbial community at 37 °C (Figure 4). Increasing the FBR temperature to 55 °C resulted in
 365 a shift of the active microbial community towards the *Thermoanaerobacterium* genus (>90% of the
 366 relative abundance).

367



368

369 **Figure 4.** Relative abundance of the active microbial community, classified at genus level, obtained
 370 by MiSeq sequencing analysis of the 16S rRNA from biofilm-containing activated carbon samples,
 371 reverse transcribed to 16S cDNA. “Other” refers to the sum of genus with a relative abundance < 1%.

372

373 4. Discussion

374 4.1 Thermophilic H₂ production and microbial community dynamics

375 The significantly higher and more stable H₂ yield obtained when performing dark fermentation of
376 xylose under thermophilic than under mesophilic conditions (Figure 2a versus 2b) was mainly due to
377 the composition of the microbial community (Figure 3; Table 1), particularly the active microbial
378 community (Figure 4). Generally, thermophilic microorganisms yield more H₂ than mesophilic
379 species [5]. A thermophilic community dominated by *Thermoanaerobacterium*, the prevalent active
380 genus in the thermophilic FBR regardless of the temperature applied (Figure 4), has already been
381 reported to yield more H₂ than a mesophilic community dominated by *Clostridium* [33]. Furthermore,
382 thermophilic conditions are not favourable for most H₂ consuming microorganisms [44].

383

384 For all the temperatures investigated (55–70 °C), the thermophilic microbial community was
385 dominated by microorganisms closely related to *Thermoanaerobacter thermosaccharolyticum*
386 (Figure 3; Table 1). Accordingly, the genus *Thermoanaerobacterium* was prevailing in the active
387 thermophilic microbial community at 60, 65 and 70 °C (Figure 4). In the thermophilic FBR, although
388 the sample at 55 °C is missing in the active microbial community analysis (Figure 4), the DGGE
389 profile (Figure 3) and the reactor performance (Figure 2a), suggest that *Thermoanaerobacterium* was
390 also the prevalent active genus at 55 °C. In fact, even in the mesophilic FBR, *Thermoanaerobacterium*
391 became dominant upon increasing the temperature from 37 to 55 °C (Figure 4). *T.*
392 *thermosaccharolyticum* has been utilised in batch reactors to produce H₂ from xylose at various
393 temperatures, obtaining a maximum yield of about 2.2 mol H₂ mol⁻¹ xylose at 60 °C [45,46].
394 However, in this study, the highest H₂ yield was only about 1.2 mol H₂ mol⁻¹ xylose at 55 °C and
395 even 30% lower at 60 °C (Figure 2a), although DGGE profiles appear similar (Figure 3). One
396 explanation is that, in this study, the pH was set to 5.0, whereas the optimum pH for *T.*
397 *thermosaccharolyticum* is 6.5 [46]. Furthermore, Koskinen et al. [36] showed that in a mesophilic
398 H₂-producing FBR, the attached microbial community is slightly different than the suspended one,

399 which was not analysed in this study. It is thus plausible that the contribution of some H₂ producing
400 or H₂ consuming microorganism on the net H₂ yield was not considered.

401

402 In the thermophilic FBR, sequences belonging to the *Clostridium* genus were detected only at 65 °C,
403 accounting for 22% of the active microbial community (Figure 4). However, at 65 °C, *Clostridium*
404 was not detected by PCR-DGGE. A possible explanation is that the concentration of *Clostridium* was
405 under the detection limit of PCR-DGGE, but these microorganisms were particularly active at 65 °C
406 and thus detected through the RNA-level sequencing analysis [32]. The activity of *Clostridium* is
407 likely linked to the unstable H₂ yield obtained at 65 °C, as some *Clostridium* sp., such as the
408 thermophilic *C. thermoaceticum*, may oxidize sugars through competitive pathways to H₂ or can even
409 carry out homoacetogenesis [47]. The role of *Clostridium* in the xylose degradation at 65 °C could
410 be further detailed by a proteomics analysis. At 65 °C, a bacterium closely related to *Alicyclobacillus*
411 sp. appeared in the DGGE profile (Figure 3). Genera with high similarity (99%) to *Alicyclobacillus*
412 sp. have been found in a thermophilic FBR used for dark fermentation of cheese whey [48], but further
413 studies are required to understand the role of this microorganism in the anaerobic processes.

414

415 The drop and subsequent increase in H₂ yield that occurred during the first days of operation at 70
416 °C, as well as the decreased xylose removal efficiency during these days (Figure 2a and 2c) can be
417 attributed to the acclimation of the microbial community to the higher temperature. Meng et al. [49]
418 performed a proteomic study on *Thermoanaerobacter tengcongensis*, cultured at 55, 75 and 80 °C,
419 and showed the existence of temperature-dependent protein complexes, which may affect the H₂
420 yield. The stable H₂ yield obtained at 70 °C after the acclimation (Figure 2a) is due to the homogeneity
421 of the active microbial community growing on the carrier material at that temperature: > 99% of the
422 total cDNA sequences at 70 °C matched the genus *Thermoanaerobacterium* (Figure 4).

423

424 The highest yield of 1.2 mol H₂ mol⁻¹ xylose was obtained at both 55 and 70 °C, whereas the H₂ yield
425 was significantly lower (0.8 mol H₂ mol⁻¹ xylose) at 60 and 65 °C. Similarly, Yokoyama et al. [50]
426 studied, in batch, dark fermentation of cow waste in the temperature range 37–85 °C, obtaining the
427 highest H₂ production at 60 °C and 75 °C, and a lower H₂ production at 67 °C. However, their cultures
428 were dominated by *Clostridium* sp. and *Caldanaerobacter* sp. at 60 and 75 °C, respectively, in
429 contrast to this study with *Thermoanaerobacter* sp. as the dominant microorganism at both 55 and 70
430 °C.

431

432 4.2 Mesophilic H₂ production and microbial community dynamics

433 The lower H₂ yield obtained under mesophilic conditions (Figure 2b) was attributed to the microbial
434 community. The DGGE profiles obtained on days 119, 158, and 185 were similar to each other and
435 mainly composed of *Clostridium* (Figure 3; Table 1), which was also shown to be the dominant active
436 genus together with the closely related *Ruminiclostridium* genus (Figure 4). Similarly, Si et al. [51]
437 studied the microbial diversity of their mesophilic H₂ producing reactors by MiSeq sequencing,
438 reporting *Clostridiaceae* as the most abundant family. Chatellard et al. [52] showed that, in particular,
439 *Clostridium* dominated mesophilic microbial communities fermenting pentose-based substrates, as
440 was also the case in this study.

441

442 Mesophilic H₂ production was unstable (Figure 2b), likely due to the accumulation of VFAs (Figure
443 2d). At high concentrations, undissociated VFAs penetrate the cell membrane, lowering the internal
444 pH and inhibiting H₂ production [14]. In fact, the H₂ yield (as well as the acetate and butyrate
445 concentration) cyclically increased and decreased in the mesophilic FBR between days 91–185, and
446 the H₂ yield was higher when the concentration of VFAs was lower (Figure 2b and 2d). Wang et al.
447 [53] reported a decrease in H₂ yield at acetate concentrations higher than 50 mM. In this study, a drop
448 in H₂ yield occurred at acetate concentrations of 40 mM.

449

450 The significantly higher H₂ yield obtained after increasing the temperature of the mesophilic FBR
451 from 37 to 55 °C (Figure 2b) is clearly due to the shift in the active microbial community from the
452 *Clostridium* and *Ruminiclostridium* genus to the *Thermoanaerobacterium* genus (Figure 4).
453 Interestingly, the H₂ yield at 55 °C remained comparable to the one obtained at 37 °C for 13 days,
454 suggesting that the change in the dominant active community did not occur immediately upon the
455 temperature change. The production of ethanol upon exposing the microbial community to 55 °C,
456 and the subsequent shift to acetate, butyrate and H₂ production, was observed also in the first days of
457 operation in the thermophilic FBR (days 1-20, Figure 2c) and in a previous batch study with the same
458 inoculum [16]. This can be attributed to either a change in the microbial community or a gradual shift
459 from ethanol to butyrate fermentation as a response to the temperature shift [16].

460

461 4.3 The role of homoacetogenesis on mesophilic and thermophilic H₂ yield

462 A decrease in H₂ yield to below 0.2 mol H₂ mol⁻¹ xylose occurred in the mesophilic FBR on days 9,
463 16, 74, and 89 (Figure 2b). On the same days, the CO₂ concentration also decreased (File S2 in the
464 supporting material) and a peak of 35–50 mM acetate was detected within 1–2 days from the H₂
465 decrease (Figure 2d), suggesting the occurrence of homoacetogenesis. H₂ and CO₂ were likely
466 consumed to produce acetate autotrophically. Several *Clostridium* sp., which dominated the active
467 mesophilic microbial community, are known homoacetogens [54]. The causes that trigger
468 microorganisms from heterotrophic to the less energy yielding autotrophic metabolism are
469 controversial. A H₂ partial pressure > 500 Pa can favour homocetogenesis and H₂ can be
470 simultaneously produced and consumed, but radioactive label tracking techniques would be required
471 to distinguish the two processes [10]. Oh et al. [55] argued that in mixed culture fermentation, the
472 switch to autotrophic metabolism occurs only after substrate depletion. This hypothesis seems less
473 probable in the studied FBR, as xylose was fed continuously. However, it is plausible that H₂

474 producing microorganisms quickly consume the xylose, inducing the facultative bacteria to shift to
475 autotrophic metabolism.

476

477 Koskinen et al. [36] studied the microbial community dynamics over time in a mesophilic (35 °C)
478 FBR reactor inoculated with digested activated sludge and concluded that the adhesion of H₂
479 consuming microorganisms, including homoacetogens, to the carrier material may cause an unstable
480 H₂ production. Similarly to this study, Dinamarca and Bakke [56] reported a decrease from 1.5 to
481 below 0.25 mol H₂ mol⁻¹ glucose after 57 days of reactor operation at 35 °C. The authors concluded
482 that homoacetogenesis is directly correlated with the HRT and dependent on biomass density and
483 sludge age [56]. Also Luo et al. [33] argued that, even if the inoculum is pretreated, methanogenic
484 and homoacetogenic microorganisms could develop again during long-term operation. Methanogens
485 are typically inhibited by a pH below 6, while homoacetogenic bacteria are also inhibited by a pH
486 below 6, but only under thermophilic conditions [33].

487

488 In the thermophilic FBR, excluding day 161 on which a decrease in H₂ yield was attributed to the
489 increased temperature, sudden drops in H₂ yield were not observed (Figure 2a) and the acetate
490 concentration was more stable (Figure 2c). This indicates a minor role of homoacetogenesis at
491 thermophilic conditions. This is in agreement with Luo et al. [33], who reported no homoacetogenesis
492 in thermophilic (55 °C) batch incubations at pH 5.5. Their thermophilic microbial community was
493 dominated by *Thermoanaerobacter* sp., as was the case in this study.

494

495 *4.4 Comparison of H₂ production with previous studies*

496 At 55 °C, despite the HRT of only 6 hours, the H₂ yield per mol xylose added is consistent with a
497 previous batch study with same inoculum and substrate [16]. At 70 °C, however, H₂ was effectively
498 produced during FBR operation, but not in the batch incubation [16], likely due to the longer time for

499 acclimation of the biomass to the high temperature. The maximum H₂ production rate (HPR) of 282.1
500 mL H₂ h⁻¹ L⁻¹ obtained at 70 °C is among the highest reported in continuous studies on thermophilic
501 dark fermentation of sugars by mixed cultures (Table 2). This is likely due to the composition of the
502 active microbial community, dominated by an effective H₂ producer such as *Thermoanaerobacterium*
503 (Figure 4). A 12-times higher HPR (3470 mL H₂ h⁻¹ L⁻¹) has been obtained with a pure culture of *T.*
504 *thermosaccharolyticum* immobilized on heat-treated methanogenic granules [57], but the sugar
505 concentration (in terms of chemical oxygen demand) was almost 3 times higher than the concentration
506 used in this study. Furthermore, O-Thong et al. [57] obtained the maximum HPR at an HRT of only
507 1 hour, whereas in this study the HRT was set to 6 hours.

508

509

510

511

512

513

514

515

516

517

518

519

520

521

522

523

524

525

526

527 **Table 2.** Highest stable H₂ production rate (HPR) obtained by dark fermentation of simple sugars in various continuous
 528 studies conducted at high temperature (T ≥ 55°C) and using different inoculum, reactor type, pH and HRT.

Inoculum	Pretreatment	Reactor type ^a	Substrate (g COD L ⁻¹)	T (°C)	pH ^b	HRT (h)	HPR (mL H ₂ h ⁻¹ L ⁻¹)	Reference
Biomass from H ₂ -producing CSTR	-	UASB	Sucrose (11.2)	55	4.5-5.0 (nc)	3	112.5	[58]
Sludge from anaerobic digester	Heat treatment (105°C, 5 min)	UASB	Sucrose (11.2)	55	5.0-5.5 (nc)	1.5	124.2	[59]
Anaerobic sludge from previously operated reactor	Heat treatment (80°C, 60min)	FBR	Sucrose (5.0)	60	5.5 (i)	12	60.5	[60]
Sludge from H ₂ producing CSTR	-	TBR	Glucose (7.3)	60	5.5 (c)	2	980.6	[24]
<i>Thermoanaerobacter thermosaccharolyticum</i> immobilised on methanogenic granules	Heat treatment (121°C, 30min)	UASB	Sucrose (22.5)	60	5.0-5.5 (nc)	1	3470	[57]
Biomass from H ₂ -producing CSTR	-	CSTR	Xylose (1.1)	70	6.7 (nc)	72	2.6	[61]
Sludge from H ₂ producing CSTR	-	UASB	Glucose (2.1)	70	7.0 (i)	24	12.7	[25]
Methanogenic biomass from CSTR	Chemical treatment (BES) ^c	UASB	Glucose (4.8)	70	7.2 (i)	27	47.3	[62]
Anaerobic sludge from thermophilic CSTR	-	CSTR	Glucose (4.6)	70	5.5 (c)	21.6	91.7	[26]
Activated sludge	Heat treatment (90°C, 15 min)	FBR	Xylose (8.0)	70	5.0 (c)	6	282.1	This study
<i>Caldicellulosiruptor saccharolyticus</i>	-	TBR	Sucrose (11.5)	73	6.5 (c)	3-5	493.1 ^d	[63]

529 ^a Continuous stirred tank reactor (CSTR), expanded granular sludge blanket (EGSB), fluidised bed reactor (FBR),
 530 sequential batch reactor (SBR), trickling bed reactor (TRB), upflow anaerobic sludge blanket (UASB).

531 ^b The reported pH refers either to the initial pH (i) or the operation pH, which can be either controlled to a stable value (c)
 532 or not controlled (nc).

533 ^c Added to the reactor feeding.

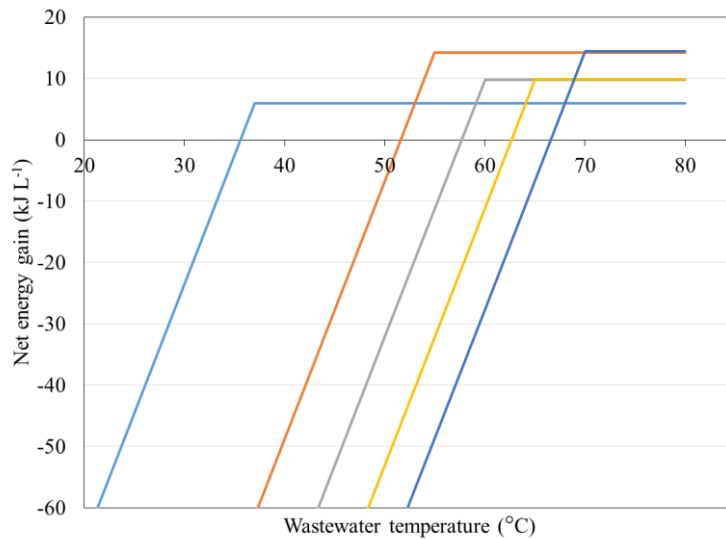
534 ^d Per L of filtering bed.

535

536 4.5 Practical implications

537 Organic carbon-rich wastewaters are produced by industries at various temperatures. The energy gain
538 from combustion of the H₂ produced and the energy required to heat the FBR to the desired
539 temperature are two important aspects to take into consideration for a proper economic analysis. For
540 a rough estimation of the effect of operation and feed wastewater temperature on energy gain of a H₂
541 producing system, a correlation between the wastewater temperature, fermentation temperature and
542 net energy gain is presented in Figure 5.

543



544

545 **Figure 5.** Effect of fermentation temperature on net energy gain from a xylose containing wastewater.
546 X-axis shows the hypothetical temperature at which the wastewater is released. The coloured lines
547 represent the net energy gain obtainable per litre of xylose (50 mM) containing wastewater treated
548 under mesophilic (37 °C) or thermophilic (55, 60, 65, 70 °C) conditions. The net energy gain was
549 calculated according to Perera et al. [22] from the average H₂ yields of the last 4 sampling points
550 collected at the various temperatures investigated in both the mesophilic and thermophilic FBR (8-
551 10 operation days).

552

553 Despite the comparatively low H₂ yield obtained (Figure 2b), dark fermentation at 37 °C is still the
554 best option to treat wastewaters produced at temperatures up to about 50 °C based on the net energy
555 gain. Thermophilic treatment at 55 °C is to be preferred for wastewaters produced at above 50 °C,
556 and the net energy gain obtained at 70 °C is comparable to the one obtained at 55 °C for wastewaters
557 produced at temperatures exceeding 70 °C (Figure 5). However, many other aspects can influence the
558 net energy gain both in a positive (heat recovery from hot wastewater, energy content of the effluent
559 and removal of pathogens) or negative (heat losses, H₂ to energy conversion efficiency and
560 maintenance and operation costs of the FBRs) way. Thermophilic processes could be advantageous
561 to treat wastewaters produced at high temperature. The data presented in this study, both on FBR
562 performance and composition of the active microbial community, helps understanding the process
563 and selecting the operation temperature in H₂ producing bioreactors depending on the temperature of
564 the waste stream to be treated. However, more research is required to further increase the net energy
565 gain. Post-treatment of the dark fermentation effluent, for recovery of value-added products such as
566 VFAs and alcohols or for further energy harvesting (e.g., H₂ production through photo-fermentation
567 or microbial electrolysis cells, methane production through anaerobic digestion or bioelectricity
568 production using microbial fuel cells) is a key factor towards process scale-up [7,64].

569

570 **5. Conclusions**

571 *Thermoanaerobacterium* dominated the thermophilic active microbial community, resulting in a
572 higher and more stable H₂ yield in the thermophilic FBR compared to the mesophilic FBR dominated
573 by *Clostridium*. Treating high temperature, xylose-containing wastewaters by thermophilic dark
574 fermentation can thus lead to a higher energy output compared to the mesophilic counterpart.
575 Temperatures of 55 and 70 °C resulted in the net maximum H₂ yield of 1.2 mol H₂ mol⁻¹ xylose,
576 whereas the competition by *Clostridium* caused unstable H₂ production at 65 °C. This study
577 contributes to the understanding of dark fermentation of xylose in FBRs, and the microorganisms

578 actively involved in the mesophilic or thermophilic process, which supports the development of high
579 rate H₂ producing bioreactors.

580

581 **Founding**

582 This work was supported by the Marie Skłodowska-Curie European Joint Doctorate (EJD) in
583 Advanced Biological Waste-To-Energy Technologies (ABWET) funded from Horizon 2020 under
584 grant agreement no. 643071.

585

586 **Conflict of interest**

587 The authors declare no conflict of interest.

588

589 **Acknowledgements**

590 The authors thank Antti Nuottajärvi (TUT, Finland) for helping in the preparation of reactor set-up
591 and Viinikanlahti municipal wastewater treatment plant (Tampere, Finland) for providing the
592 activated sludge.

593

594 **References**

- 595 [1] Hallenbeck PC, Abo-Hashesh M, Ghosh D. Strategies for improving biological hydrogen
596 production. *Bioresour Technol* 2012;110:1–9.
- 597 [2] Nikolaidis P, Poullikkas A. A comparative overview of hydrogen production processes. *Renew
598 Sustain Energy Rev* 2017;67:597–611.
- 599 [3] Arimi MM, Knodel J, Kiprop A, Namango SS, Zhang Y, Geißen S-U. Strategies for
600 improvement of biohydrogen production from organic-rich wastewater: A review. *Biomass
601 and Bioenergy* 2015;75:101–18.
- 602 [4] Van Groenestijn JW, Hazewinkel JHO, Nienoord M, Bussmann PJT. Energy aspects of

- 603 biological hydrogen production in high rate bioreactors operated in the thermophilic
604 temperature range. Int J Hydrogen Energy 2002;27:1141–7.
- 605 [5] Lee D-J, Show K-Y, Su A. Dark fermentation on biohydrogen production: Pure culture.
606 Bioresour Technol 2011;102:8393–402.
- 607 [6] Vipotnik Z, Jessen JE, Scully SM, Orlygsson J. Effect of culture conditions on hydrogen
608 production by *Thermoanaerobacter* strain AK68. Int J Hydrogen Energy 2016;41:181–9.
- 609 [7] Ghimire A, Frunzo L, Pirozzi F, Trably E, Escudie R, Lens PNL, et al. A review on dark
610 fermentative biohydrogen production from organic biomass: Process parameters and use of
611 by-products. Appl Energy 2015;144:73–95.
- 612 [8] Pawar SS, van Niel EWJ. Thermophilic biohydrogen production : how far are we? Appl
613 Microbiol Biotechnol 2013;97:7999–8009.
- 614 [9] Thauer RK, Jungermann K, Decker K. Energy Conservation in Chemotrophic Anaerobic
615 Bacteria. Bacteriol Rev 1977;41:100–80.
- 616 [10] Saady NMC. Homoacetogenesis during hydrogen production by mixed cultures dark
617 fermentation: Unresolved challenge. Int J Hydrogen Energy 2013;38:13172–91.
- 618 [11] Angenent LT, Karim K, Al-dahhan MH, Wrenn BA, Domı R. Production of bioenergy and
619 biochemicals from industrial and agricultural wastewater. Trends Biotechnol 2004;22:477–85.
- 620 [12] Li C, Fang HHP. Fermentative Hydrogen Production From Wastewater and Solid Wastes by
621 Mixed Cultures. Crit Rev Environ Sci Technol 2007;37:1–39.
- 622 [13] Hüsemann MHW, Papoutsakis ET. Solventogenesis in *Clostridium Acetobutylicum*
623 Fermentations Related to Carboxylic Acid and Proton Concentrations. Biotechnol Bioeng
624 1988;32:843–52.
- 625 [14] Bundhoo MAZ, Mohee R. Inhibition of dark fermentative bio-hydrogen production: A review.
626 Int J Hydrogen Energy 2016;41:6713–33.
- 627 [15] Pradhan N, Dipasquale L, d’Ippolito G, Panico A, Lens PNL, Esposito G, et al. Hydrogen

- 628 Production by the Thermophilic Bacterium *Thermotoga neapolitana*. Int J Mol Sci
629 2015;16:12578–600.
- 630 [16] Dessì P, Lakaniemi A-M, Lens PNL. Biohydrogen production from xylose by fresh and
631 digested activated sludge at 37, 55 and 70 °C. Water Res 2017;115:120–9.
- 632 [17] Ratkowsky DA, Olley J, McMeekin TA, Ball A. Relationship Between Temperature and
633 Growth Rate of Bacterial Cultures. J Bacteriol 1982;149:1–5.
- 634 [18] Verhaart MRA, Bielen AAM, van der Oost J, Stams AJM, Kengen SWM. Hydrogen
635 production by hyperthermophilic and extremely thermophilic bacteria and archaea:
636 mechanisms for reductant disposal. Environ Technol 2010;31:993–1003.
- 637 [19] Kargi F, Eren NS, Ozmihci S. Bio-hydrogen production from cheese whey powder (CWP)
638 solution: Comparison of thermophilic and mesophilic dark fermentations. Int J Hydrogen
639 Energy 2012;37:8338–42.
- 640 [20] Zheng H-S, Guo W-Q, Yang S-S, Feng X-C, Du J-S, Zhou X-J, et al. Thermophilic hydrogen
641 production from sludge pretreated by thermophilic bacteria: Analysis of the advantages of
642 microbial community and metabolism. Bioresour Technol 2014;172:433–7.
- 643 [21] Kumar G, Sivagurunathan P, Sen B, Mudhoo A, Davila-Vazquez G, Wang G, et al. Research
644 and development perspectives of lignocellulose-based biohydrogen production. Int Biodeterior
645 Biodegradation 2017;119:225–38.
- 646 [22] Perera KRJ, Ketheesan B, Gadhamshetty V, Nirmalakhandan N. Fermentative biohydrogen
647 production : Evaluation of net energy gain. Int J Hydrogen Energy 2010;35:12224–33.
- 648 [23] Suvilampi J, Lepistö R, Rintala J. Biological treatment of pulp and paper mill process and
649 wastewaters under thermophilic conditions – A review. Pap Timber 2001;83:320–5.
- 650 [24] Oh Y-K, Kim SH, Kim M-S, Park S. Thermophilic biohydrogen production from glucose with
651 trickling biofilter. Biotechnol Bioeng 2004;88:690–8.
- 652 [25] Zheng H, Zeng RJ, Angelidaki I. Biohydrogen Production From Glucose in Upflow Biofilm

- 653 Reactors With Plastic Carriers Under Extreme Thermophilic Conditions (70°C). *Biotechnol*
654 *Bioeng* 2008;100:1034–8.
- 655 [26] Zhang F, Chen Y, Dai K, Zeng RJ. The chemostat study of metabolic distribution in extreme-
656 thermophilic (70 °C) mixed culture fermentation. *Appl Microbiol Biotechnol* 2014;98:10267–
657 73.
- 658 [27] Cavalcante de Amorim EL, Barros AR, Rissato Zamariolli Damianovic MH, Silva EL.
659 Anaerobic fluidized bed reactor with expanded clay as support for hydrogen production
660 through dark fermentation of glucose. *Int J Hydrogen Energy* 2009;34:783–90.
- 661 [28] Karadag D, Puhakka JA. Effect of changing temperature on anaerobic hydrogen production
662 and microbial community composition in an open-mixed culture bioreactor. *Int J Hydrogen*
663 *Energy* 2010;35:10954–9.
- 664 [29] Etchebehere C, Castelló E, Wenzel J, del Pilar Anzola-Rojas M, Borzacconi L, Buitrón G, et
665 al. Microbial communities from 20 different hydrogen-producing reactors studied by 454
666 pyrosequencing. *Appl Microbiol Biotechnol* 2016;100:3371–84.
- 667 [30] Nitipan S, Mamimin C, Intrasungkha N, Birkeland NK, O-Thong S. Microbial community
668 analysis of thermophilic mixed culture sludge for biohydrogen production from palm oil mill
669 effluent. *Int J Hydrogen Energy* 2014;39:19285–93.
- 670 [31] Zhang F, Yang J-H, Dai K, Ding Z-W, Wang L-G, Li Q-R, et al. Microbial dynamics of the
671 extreme-thermophilic (70 °C) mixed culture for hydrogen production in a chemostat. *Int J*
672 *Hydrogen Energy* 2016;41:11072–80.
- 673 [32] De Vrieze J, Regueiro L, Props R, Vilchez-Vargas R, Jáuregui R, Pieper DH, et al. Presence
674 does not imply activity: DNA and RNA patterns differ in response to salt perturbation in
675 anaerobic digestion. *Biotechnol Biofuels* 2016;9:244.
- 676 [33] Luo G, Karakashev D, Xie L, Zhou Q, Angelidaki I. Long-Term Effect of Inoculum
677 Pretreatment on Fermentative Hydrogen Production by Repeated Batch Cultivations:

- 678 Homoacetogenesis and Methanogenesis as Competitors to Hydrogen Production. *Biotechnol*
679 *Bioeng* 2011;108:1816–27.
- 680 [34] Kinnunen V, Ylä-Outinen a., Rintala J. Mesophilic anaerobic digestion of pulp and paper
681 industry biosludge–long-term reactor performance and effects of thermal pretreatment. *Water*
682 *Res* 2015;87:105–11.
- 683 [35] Mäkinen AE, Nissilä ME, Puhakka JA. Dark fermentative hydrogen production from xylose
684 by a hot spring enrichment culture. *Int J Hydrogen Energy* 2012;37:12234–40.
- 685 [36] Koskinen PEP, Kaksonen AH, Puhakka JA. The Relationship Between Instability of H₂
686 Production and Compositions of Bacterial Communities Within a Dark Fermentation
687 Fluidized-Bed Bioreactor. *Biotechnol Bioeng* 2006;97:742–58.
- 688 [37] Hall T. BioEdit: a user-friendly biological sequence alignment editor and analysis program for
689 Windows 95/98/NT. *Nucleic Acids Symp Ser* 1999;41:95–8. doi:citeulike-article-id:691774.
- 690 [38] Altschul SF, Gish W, Miller W, Myers EW, Lipman DJ. Basic local alignment search tool. *J*
691 *Mol Biol* 1990;215:403–10.
- 692 [39] Griffiths RI, Whiteley AS, O’Donnell AG, Bailey MJ. Rapid Method for Coextraction of DNA
693 and RNA from Natural Environments for Analysis of Ribosomal DNA- and rRNA-Based
694 Microbial Community Composition. *Appl Environ Microbiol* 2000;66:5488–91.
- 695 [40] Caporaso JG, Lauber CL, Walters WA, Berg-Lyons D, Lozupone CA, Turnbaugh PJ, et al.
696 Global patterns of 16S rRNA diversity at a depth of millions of sequences per sample. *Proc*
697 *Natl Acad Sci U S A* 2011;108:4516–22.
- 698 [41] Schloss PD, Westcott SL, Ryabin T, Hall JR, Hartmann M, Hollister EB, et al. Introducing
699 mothur: open-source, platform-independent, community-supported software for describing
700 and comparing microbial communities. *Appl Environ Microbiol* 2009;75:7537–41.
- 701 [42] Kozich JJ, Westcott SL, Baxter NT, Highlander SK, Schloss PD. Development of a dual-index
702 sequencing strategy and curation pipeline for analyzing amplicon sequence data on the miseq

- 703 illumina sequencing platform. *Appl Environ Microbiol* 2013;79:5112–20.
- 704 [43] Box GEP, Holohan R, Scott E. *Statistics for experimenters: an introduction to design, data*
705 *analysis, and model building.* John Wiley and sons; 1978.
- 706 [44] Hasyim R, Imai T, Reungsang A, O-Thong S. Extreme-thermophilic biohydrogen production
707 by an anaerobic heat treated digested sewage sludge culture. *Int J Hydrogen Energy*
708 2011;36:8727–34.
- 709 [45] Khamtib S, Reungsang A. Biohydrogen production from xylose by *Thermoanaerobacterium*
710 *thermosaccharolyticum* KKU19 isolated from hot spring sediment. *Int J Hydrogen Energy*
711 2012;37:12219–28.
- 712 [46] Ren N, Cao G, Wang A, Lee D, Guo W, Zhu Y. Dark fermentation of xylose and glucose mix
713 using isolated *Thermoanaerobacterium thermosaccharolyticum* W16. *Int J Hydrogen Energy*
714 2008;33:6124–32.
- 715 [47] Koesnandar, Nishio N, Nagai S. Effects of Trace Metal Ions on the Growth, Homoacetogenesis
716 and Corrinoid Production by *Clostridium thermoaceticum*. *J Ferment Bioeng* 1991;71:181–5.
- 717 [48] Ottaviano LM, Ramos LR, Botta LS, Amâncio Varesche MB, Silva EL. Continuous
718 thermophilic hydrogen production from cheese whey powder solution in an anaerobic fluidized
719 bed reactor: Effect of hydraulic retention time and initial substrate concentration. *Int J*
720 *Hydrogen Energy* 2017;42:4848–60.
- 721 [49] Meng B, Qian Z, Wei F, Wang W, Zhou C, Wang Z, et al. Proteomic analysis on the
722 temperature-dependent complexes in *Thermoanaerobacter tengcongensis*. *Proteomics*
723 2009;9:3189–200.
- 724 [50] Yokoyama H, Waki M, Moriya N, Yasuda T, Tanaka Y, Haga K. Effect of fermentation
725 temperature on hydrogen production from cow waste slurry by using anaerobic microflora
726 within the slurry. *Appl Microbiol Biotechnol* 2007;74:474–83.
- 727 [51] Si B, Liu Z, Zhang Y, Li J, Xing X-H, Li B, et al. Effect of reaction mode on biohydrogen

- 728 production and its microbial diversity. *Int J Hydrogen Energy* 2015;40:3191–200.
- 729 [52] Chatellard L, Trably E, Carrère H. The type of carbohydrates specifically selects microbial
730 community structures and fermentation patterns. *Bioresour Technol* 2016;221:541–9.
- 731 [53] Wang B, Wan W, Wang J. Inhibitory effect of ethanol, acetic acid, propionic acid and butyric
732 acid on fermentative hydrogen production. *Int J Hydrogen Energy* 2008;33:7013–9.
- 733 [54] Ryan P, Forbes C, Colleran E. Investigation of the diversity of homoacetogenic bacteria in
734 mesophilic and thermophilic anaerobic sludges using the formyltetrahydrofolate synthetase
735 gene. *Water Sci Technol* 2008;57:675–80.
- 736 [55] Oh S-E, Van Ginkel S, Logan BE. The Relative Effectiveness of pH Control and Heat
737 Treatment for Enhancing Biohydrogen Gas Production. *Environ Sci Technol* 2003;37:5186–
738 90.
- 739 [56] Dinamarca C, Bakke R. Apparent hydrogen consumption in acid reactors: observations and
740 implications. *Water Sci Technol* 2009;59:1441–7.
- 741 [57] O-Thong S, Prasertsan P, Karakashev D, Angelidaki I. High-rate continuous hydrogen
742 production by *Thermoanaerobacterium thermosaccharolyticum* PSU-2 immobilized on heat-
743 pretreated methanogenic granules. *Int J Hydrogen Energy* 2008;33:6498–508.
- 744 [58] Keskin T, Giusti L, Azbar N. Continuous biohydrogen production in immobilized biofilm
745 system versus suspended cell culture. *Int J Hydrogen Energy* 2012;37:1418–24.
- 746 [59] Keskin T, Aksöyek E, Azbar N. Comparative analysis of thermophilic immobilized
747 biohydrogen production using packed materials of ceramic ring and pumice stone. *Int J*
748 *Hydrogen Energy* 2011;36:15160–7.
- 749 [60] Lutpi NA, Md Jahim J, Mumtaz T, Harun S, Abdul PM. Batch and continuous thermophilic
750 hydrogen fermentation of sucrose using anaerobic sludge from palm oil mill effluent via
751 immobilisation technique. *Process Biochem* 2016;51:297–307.
- 752 [61] Kongjan P, Min B, Angelidaki I. Biohydrogen production from xylose at extreme thermophilic

- 753 temperatures (70 degrees C) by mixed culture fermentation. *Water Res* 2009;43:1414–24.
- 754 [62] Kotsopoulos TA, Zeng RJ, Angelidaki I. Biohydrogen production in granular up-flow
755 anaerobic sludge blanket (UASB) reactors with mixed cultures under hyper-thermophilic
756 temperature (70°C). *Biotechnol Bioeng* 2006;94:296–302.
- 757 [63] Van Groenestijn JW, Geelhoed JS, Goorissen HP, Meesters KPM, Stams AJM, Claassen PAM.
758 Performance and Population Analysis of a Non-Sterile Trickle Bed Reactor Inoculated With
759 *Caldicellulosiruptor saccharolyticus*, a Thermophilic Hydrogen Producer. *Biotechnol Bioeng*
760 2009;102:1361–7.
- 761 [64] Sharma Y, Li B. Optimizing energy harvest in wastewater treatment by combining anaerobic
762 hydrogen producing biofermentor (HPB) and microbial fuel cell (MFC). *Int J Hydrogen*
763 *Energy* 2010;35:3789–97.
- 764